

TRANSIENT ANALYSIS OF THE SQUIRREL CAGE INDUCTION MOTOR

Qurban Ali Shah Syed^{*1}, Muharam Ali Shah², Manthar Ali³, Zuhebullah Soomro⁴^{*1,4}Department of Electrical Engineering, The University of Larkano, Larkana, Pakistan²Department of Electronics and Power Engineering, PNEC-NUST, Karachi, Pakistan³Department of Mechanical Engineering, The University of Larkano, Larkana, Pakistan^{*1}qurban.syed@uolrk.edu.pk, ²muhamam.shah786@gmail.com, ³manthar.khoso@gmail.com,⁵soomrozohaib17@gmail.comDOI: <https://doi.org/10.5281/zenodo.17481227>**Keywords**

asynchronous machine, dynamic condition monitoring, finite element analysis, induction motor, squirrel cage rotor, transient magnetic analysis.

Article History

Received: 10 September 2025

Accepted: 16 October 2025

Published: 30 October 2025

Copyright @Author

Corresponding Author: *
Qurban Ali Shah Syed**Abstract**

This research paper provides a comprehensive electromagnetic transient analysis of the squirrel cage induction motor (IM), using the finite element analysis (FEA) method. The dynamic behavior of the squirrel cage IMs under various operational conditions, including startup, rated load, and fault scenarios, are considered and computed using the 2D FEA. Although, the steady state electromagnetic analysis by the corresponding author evaluates the squirrel cage IM's performance at different rotor positions, supplied voltages, rotor slips, and at different operating conditions of the no-load and the blocked-rotor cases [Syed, Q.A.S., et al. 2025], it fails in evaluating the dynamic responses influenced by magnetic field harmonics and rotor motion, which are critical for accurate motor design and performance prediction. To overcome the limitations of steady-state electromagnetic analysis, parameters such as electromagnetic torque, phase currents, and speed during dynamic conditions of the squirrel cage IM are determined by using the transient electromagnetic analysis. The squirrel cage IM's dynamic behavior is simulated using the 2D FEA to analyze its electromagnetic behavior from a no-load startup, through the application of rated drag torque, and finally under fault conditions, such as a single-phase short-circuit. The time-evolved quantities, such as, current, electromagnetic torque, and speed are observed and analyzed, during these three dynamic conditions of no-load startup, rated load and under fault conditions. The framework for predicting the transient performance of squirrel cage IM is offered, offering insights into their stability and response characteristics under dynamic and fault conditions.

1. INTRODUCTION

Induction motors (IMs) are the base to industrial applications due to their robustness, reliability, and cost effectiveness, and are the most widely used electric motors, accounting for over 85% of applications involving rotating apparatus and consuming more than 60% of industrial electricity in developed countries [El-Shahat, A. et al., 2023], [Syed, Q.A.S. et al., 2025]. The squirrel cage type IMs are

particularly favored for their simplicity, low maintenance, and high efficiency compared to the wound rotor type IMs [Lipo, T.A. 2017]. There are two main types of IMs, considering the rotor type, such as, a squirrel-cage IM and wound rotor IM. A squirrel cage IM is simple and rugged, whereas a wound-rotor IM provides better control over torque and speed [Boldea, I., et al. 2010].

A squirrel cage IM has two main parts, the stator and the rotor, as shown in Figure 1. The stator is stationary and consists of laminated electrical steel sheets to reduce the iron loss [Boldea, I., et al. 2010], [Kovács, K. 2022]. When a three-phase ac voltage supply is applied to the stator, it produces a rotating magnetic field. This rotating field cuts the stationary rotor bars of the squirrel cage IM, inducing electromotive force (EMF) due to Faraday's law of induction [Lipo, T.A. 2017]. The rotor of a squirrel cage IM always lags behind the rotating magnetic field; hence the term asynchronous motor is also used for the IM [Boldea, I., et al. 2010], [Bleizgys, V., et al. 2010]. A squirrel cage IM's rotor bars are short-circuited through end rings, flowing current induces their own magnetic field, and the interaction between the stator's rotatory field and the induced rotor field develops the desired electromagnetic torque, responsible for running the squirrel cage IM under load conditions.

Squirrel cage IMs have a robust design requiring less maintenance, and do not require brushes or commutators, which are common failure points [Boldea, I., et al. 2010]. Due to the reliability, cost-effectiveness, and ease of maintenance of the IMs, these are used across various sectors, including industrial, commercial, and domestic applications, such as pumps, fans, conveyors, household appliances, and even electric vehicles (EVs) [Azab, M. 2025], [Ahmed, S., et al. 2025]. Understanding the operation and torque-speed characteristics of these

motors is a key to optimizing performance and efficiency, particularly in complex industrial environments.

Although, the transient electromagnetic behavior in IMs is analyzed by analytical, numerical or combination of both the methods, the finite element analysis (FEA) numerical method has been employed to determine the electromagnetic fields within the squirrel cage IM [Balamurugan, S., et. al., 2004], [Zhang, D., et. al., 2018]. The transient electromagnetic analysis provides deeper insights for the design, optimization, and performance evaluation of the squirrel cage IMs [Altair Engineering, Inc. 2025].

Initial rotor position is crucial for accurate transient initialization, and it is determined in [Syed, Q.A.S., et. al. 2025] during the steady state analysis of the squirrel cage IM, by parameterized magneto-harmonic analysis across different rotor positions to establish the position where electromagnetic torque equals its average value. Transient magnetic analysis of the squirrel cage IM at rated speed is carried out to study the transient behavior of electromagnetic torque, and rotor bar and stator currents under rated speed conditions [Di Nardo, M., et al. 2020]. However, influence of the real working conditions on the dynamic performance of the squirrel cage IM are analyzed at a no-load startup, followed by the application of rated load, and also with a single-phase short-circuit fault, observing the time evolution of main quantities.

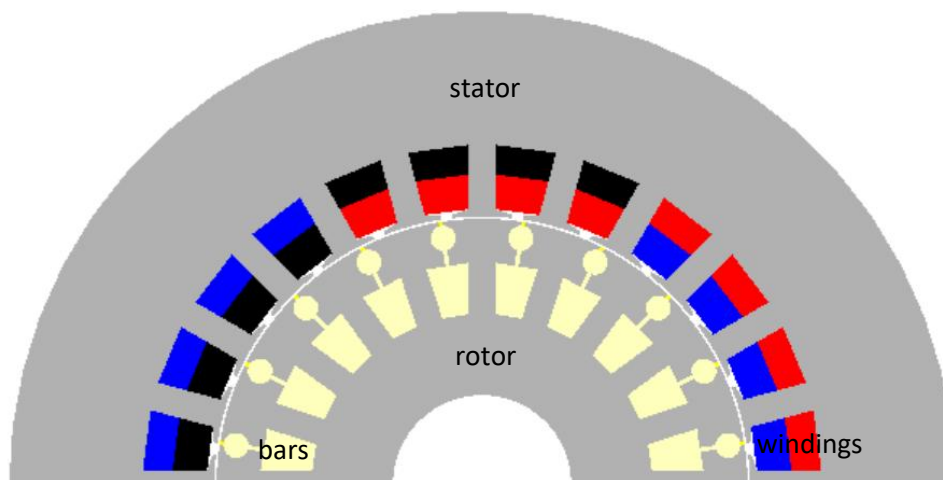


Figure 1: Three-phase squirrel cage IM.

2. SQUIRREL CAGE INDUCTION MOTOR

The squirrel cage IM has 2 poles, 24 stator slots for the stator coil winding and 20 rotor slots for the rotor bars. Stator winding is a double layer lap winding scheme, whereas, rotor of the IM is double squirrel cage, as shown in Figure 1. Rotor bars of the squirrel cage IM are of cast aluminum, and are interconnected by end rings, which help in the formation of the squirrel cage. This construction minimizes losses and enhances performance, under

high-speed conditions. The stator winding uses copper conductors and is arranged in a two-layer configuration.

The geometrical design specifications of the squirrel cage IM are provided in Table 1. The outer diameter of the squirrel cage IM is 212 mm, while the average airgap diameter of the squirrel cage IM is 118.5 mm, and the shaft diameter is 40 mm. The axial length without the end winding length of the squirrel cage IM is 125 mm.

Table 1: Geometrical specifications of the squirrel cage IM.

Symbol	Item	Value
P	Rated load power	7.5 kW
V	Supply voltage	380 V
f	Frequency	50 Hz
S	Stator slots	24
R_{so}	Sator outer radius	106 mm
R_{ro}	Rotor outer radius	69.5 mm
R_s	Shaft radius	20 mm
g	Airgap	0.5 mm
L	Total axial length	125 mm
N	Stator winding turns per phase	208



3. METHODOLOGY

The FEA method is utilized to simulate the squirrel cage induction motor (IM), for analyzing the motor's output characteristics under dynamic working conditions. The squirrel cage IM's geometry is defined using the Altair manual [Altair Engineering, Inc. 2025], then meshed into fine elements. The meshing must be fine, especially in areas like the rotor bars of the squirrel cage IM and the airgap where electromagnetic interactions are most significant. The airgap is divided into two parts, i.e., rotating airgap and stationary airgap, and fine meshing is done at the line dividing both the airgap regions. To reduce the computation time of the 2D FEA, symmetry and periodicity of the squirrel cage IM is determined and the relevant boundary conditions are applied before solving the model.

To solve the dynamic working conditions of the squirrel cage IM, a 2D magneto-harmonic and transient magnetic simulations using Altair Flux is utilized. The process includes defining the solver

applications as the transient magnetic 2D, creating and modifying mechanical sets for both rotor and stator, and configuring detailed electric circuits. The physical properties like specific materials are chosen from the material's manager and assigned to their respective regions of the squirrel cage IM, ensuring the material properties concerned. Stator windings and their connections, rotor bars and their connections are assigned to the respective electrical circuit components.

Initial rotor position is crucial for accurate transient initialization, and it is determined in [Syed, Q.A.S., et. al. 2025] during the steady state analysis of the squirrel cage IM, by parameterized magneto-harmonic analysis across different rotor positions to establish the position where electromagnetic torque equals its average value. Transient magnetic analysis of the squirrel cage IM at rated speed is carried out to study the transient behavior of electromagnetic torque, and rotor bar and stator currents under rated speed conditions. However, influence of the real

working conditions on the dynamic performance of the squirrel cage IM are analyzed at a no-load startup, followed by the application of rated load, and also with a single-phase short-circuit fault, observing the time evolution of main quantities.

4. TRANSIENT ANALYSIS AT RATED SPEED

4.1 Electromagnetic torque

The electromagnetic torque of the squirrel cage IM against the angular position of the rotor over time is computed and displayed in Figure 2. It is important to verify the initial electromagnetic torque at a slip of

0.032 from this transient model by the steady-state model of the squirrel cage IM presented in [Syed, Q.A.S., et. al. 2025]. The slip of 0.032 provides the nominal power of the squirrel cage IM, and the steady-state model of the squirrel cage IM has yielded an electromagnetic torque of 24.13 N.m, while the transient model's electromagnetic torque is 26.2 N.m. The electromagnetic torque stabilizes over time under rated speed conditions, considering the magnetic field harmonics due to stator and rotor slotting and rotor motion, and dynamic performance of the squirrel cage IM.

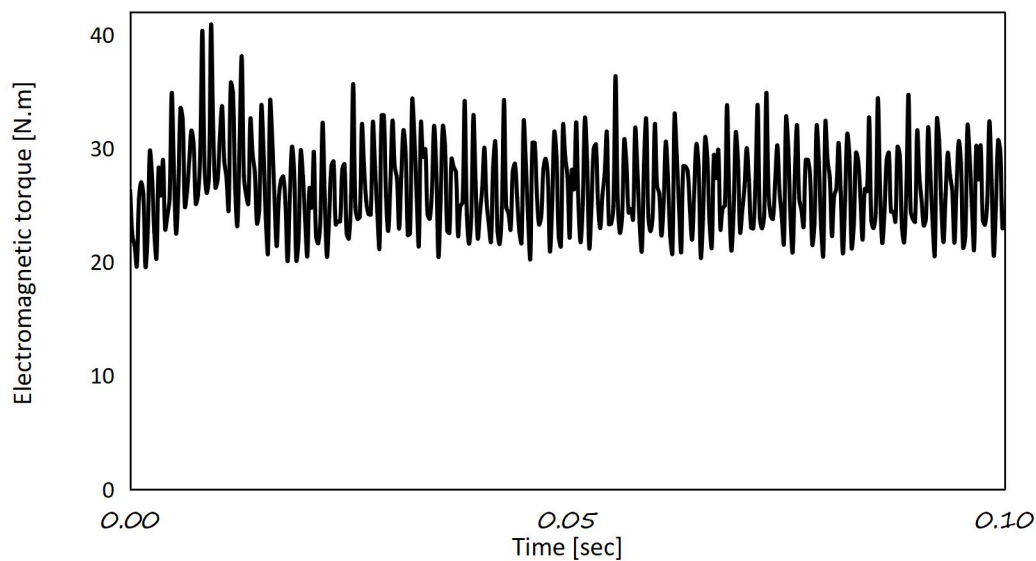


Figure 2: Electromagnetic torque of the squirrel cage IM stabilizes over time.

4.2 Current characteristics of the rotor bars

This analysis computes and displays the current values in the rotor bars of the squirrel cage IM, as shown in Figure 3. Similar to the electromagnetic torque, at $t = 0$ sec from the transient model is compared with the steady-state model of the squirrel cage IM for a slip of 0.032. As, the steady-state model has 512 A current in the rotor bar of the squirrel cage IM with phase of 3.0744 radians. Thus, the initial value for the current in the rotor bar of the

transient squirrel cage IM is 34.78 A. The dynamic response of the squirrel cage IM contains oscillations due to the alternating current flowing through the rotor bars, which is induced by the rotating magnetic field of the stator. The transient analysis for the current provides crucial insights into the electrical stresses and performance of the rotor bars during the dynamic operation at rated speed of the squirrel cage IM.

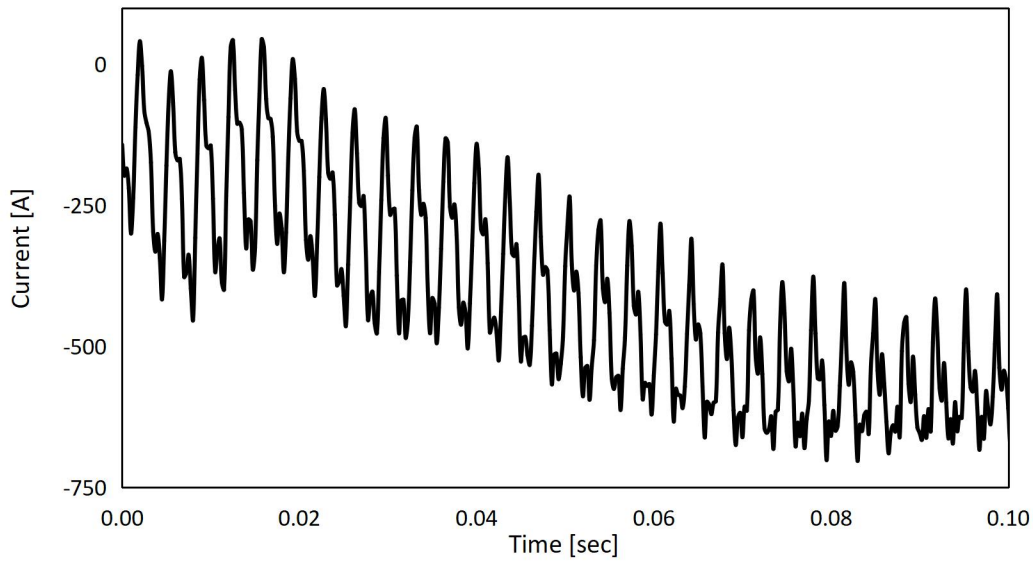


Figure 3: Current characteristics of a squirrel cage rotor bar at rated speed.

4.3 Current characteristics of the stator windings

The stator current values are also computed during the transient analysis of the squirrel cage IM, and results are displayed in Figure 4. At a slip of 0.032, and the current during the steady-state model of the squirrel cage IM is 11.969 A with a phase angle of

2.547 radians, thus, the initial transient value of the current in a stator winding is 6.13 A. Thus, the transient analysis of the stator winding's current characteristics is quite important to study the dynamic behavior of a squirrel cage IM under rated speed conditions.

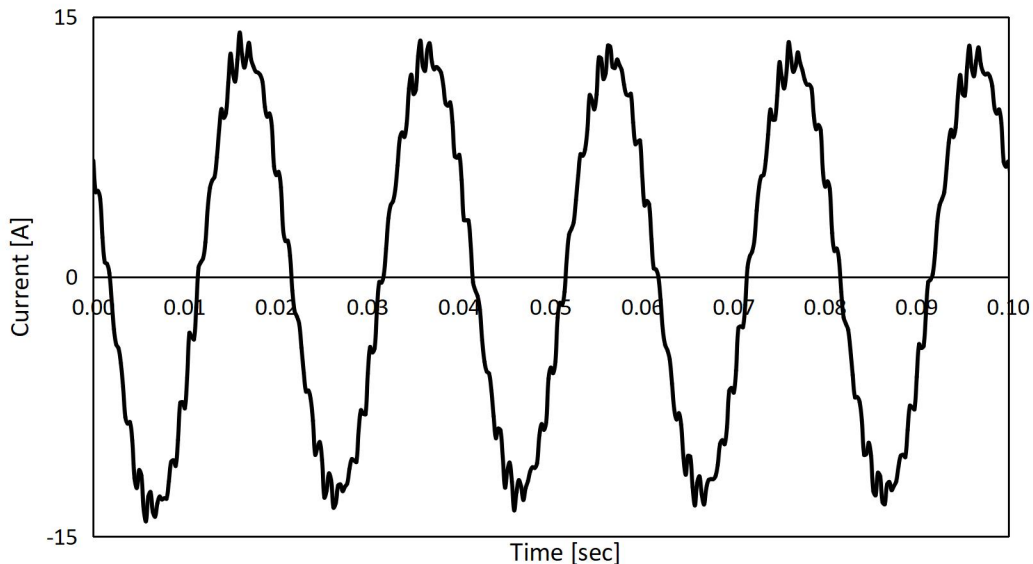


Figure 4: Current characteristics of a stator winding of phase A of squirrel cage IM.

5. TRANSIENT ANALYSIS AT REAL WORKING CONDITIONS

The transient magnetic computation of the squirrel cage IM aims to provide a comprehensive understanding of the motor's dynamic response under realistic operating conditions, including starting, loading, and fault scenarios. From 0 to 0.4 sec the squirrel cage IM undergoes a no-load starting phase, thus the transient analysis using the 2D FEA provides startup characteristics under no-load conditions. After the no-load starting phase, a rated drag torque is applied to the squirrel cage IM, and the loading occurs at $t=0.4$ sec. and the motor transitions from the no-load to its operational load. Later, the single-phase short-circuit between one phase and neutral is considered at 0.6 sec. demonstrating the squirrel cage IM's transient response to an electrical fault.

5.1 Current characteristics

During these three different phases, the current in the three phases of the squirrel cage IM is displayed

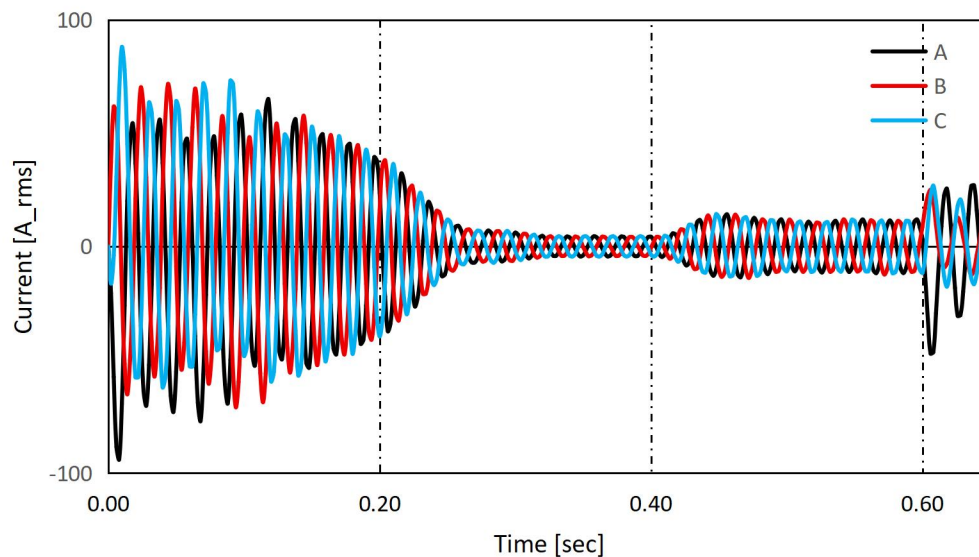


Figure 5: Three phase current characteristics during a real working condition of the squirrel cage IM.

5.2 Magnetic flux density distribution

The magnetic flux density in the stator and rotor of the squirrel cage IM during the real operating conditions is shown in Figure 6. During the startup, the current is high and the induced flux density is quite high, as shown in Figure 6 (a). When the

current stabilizes the flux density distribution in the stator and rotor core of the squirrel cage IM is provided in Figure 6 (b). When the drag torque is applied, the current increases more than the stabilized no load current, therefore, flux density is higher than the Fig. 6 (b), as shown in Figure 6 (c).

When a single phase is short circuited and fault occurs, the current has oscillations and its magnitude is higher than the no load stabilized condition as well

as applied load condition, therefore, flux density in the stator and rotor of the squirrel cage IM is higher, as shown in Figure 6 (d).

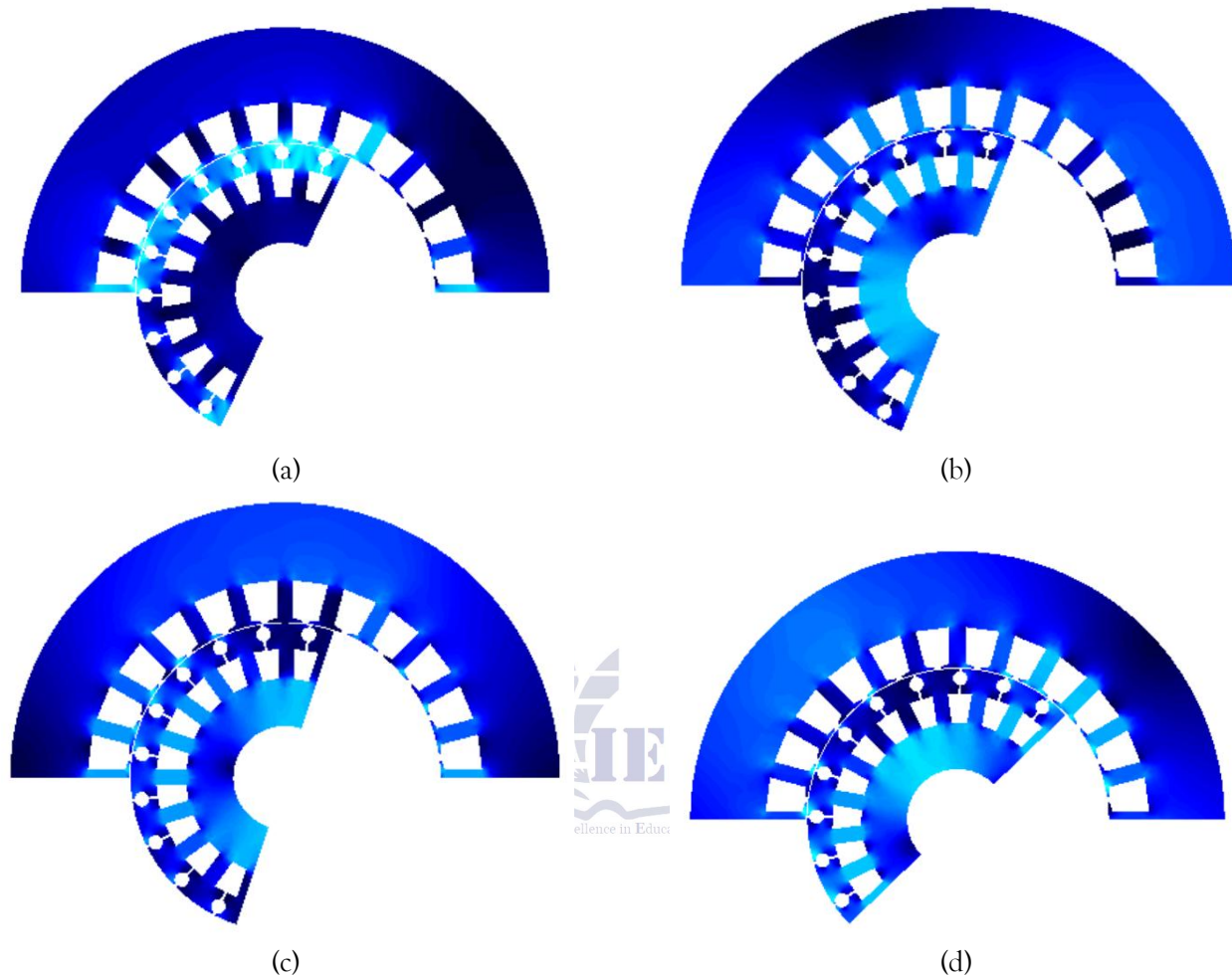


Figure 6: Flux density distribution in the stator and rotor of the squirrel cage IM, during the real operating conditions, where, dark color represents low flux density of 0T, whereas, light color is 3.15T: (a) No load condition with inrush current at 0.044 sec., (b) No load condition with stabilized current at 0.35 sec., (c) Load condition at 0.514 sec., (d) Fault condition at 0.636 sec.

5.3 Speed characteristics

The acceleration during a no-load starting, the change in speed when load is applied, and the impact of the short-circuit on the squirrel cage IM's rotational speed, is shown in Figure 7. Thus, it provides insight into the squirrel cage IM's dynamic response upon its speed under the real working conditions. During the no load starting, the squirrel cage IM is accelerating from a standstill without any external load, and the speed rapidly increases and

then stabilizes as the motor reaches its no-load operating speed. Following the no-load starting phase, the change in speed corresponds to the application of a rated drag torque at $t = 0.4$ sec., and the squirrel cage IM's speed decreases slightly and then stabilizes at a new operating point under load. However, after 0.6 sec. the squirrel cage IM depicts its speed response to a fault operational condition, and the speed fluctuates, reflecting the impact of the electrical fault on the motor's rotational dynamics.

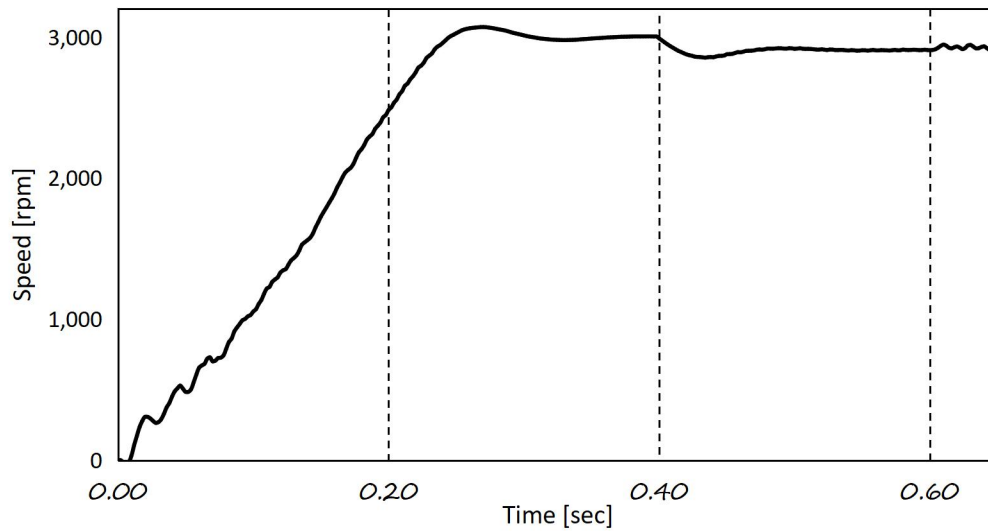


Figure 7: Speed characteristics of the squirrel cage IM, during a real working condition.

5.4 Electromagnetic torque characteristics

The electromagnetic torque of the squirrel cage IM under real working conditions, during no-load starting from 0 to 0.4 sec, under load, and the transient behavior during the short-circuit condition from 0.6 sec., is shown in Figure 8. During the no load starting condition, the electromagnetic torque fluctuates heavily as the squirrel cage IM accelerates and once the speed builds up, the electromagnetic torque stabilizes too, as it approaches its no-load operating point. At 0.4 sec., a significant change in the electromagnetic torque is

observed, corresponding to the application of a rated drag torque. Thus, the electromagnetic torque of the squirrel cage IM increases to overcome the applied load, leading to a new operating state. However, at 0.6 sec. a single-phase short-circuit between one phase and neutral of the stator winding of the squirrel cage IM occurs. During this period, the electromagnetic torque exhibits severe oscillations and potentially drops significantly, reflecting the squirrel cage IM's struggle to maintain operation under the fault condition.

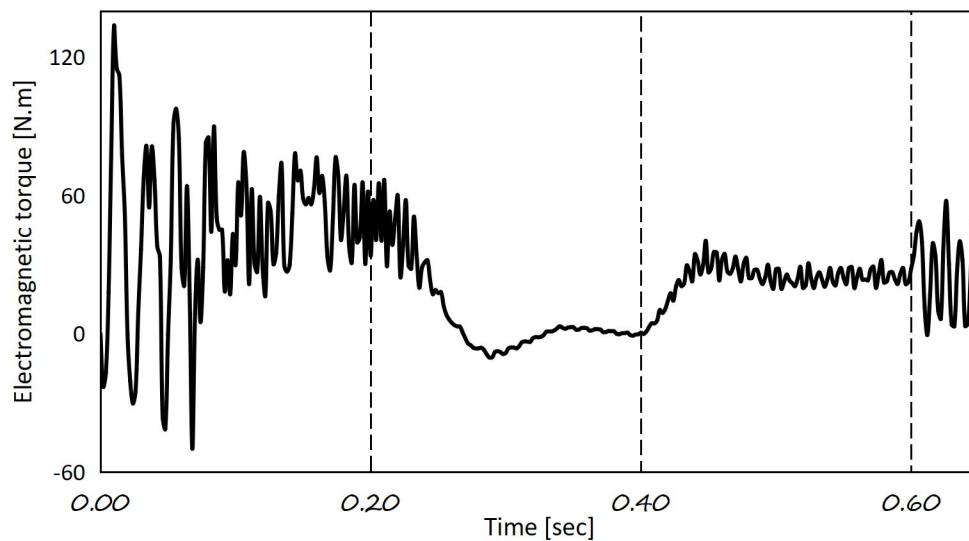


Figure 8: Electromagnetic torque characteristics of the squirrel cage IM, during real working conditions.

Thus, the transient analysis of the squirrel cage IM's electromagnetic torque output highlights its dynamic response to startup, sudden loading, and electrical fault scenarios, which are critical for understanding the motor's robustness and control requirements in real-world applications.

6. CONCLUSION:

The transient analysis in this research paper focuses on the dynamic behavior of the squirrel cage IM under various operating conditions, including startup, rated load, and fault conditions, and provides a comprehensive understanding of the IM's dynamic performance. There is a slight difference in initial characteristics of the squirrel cage IM between the steady-state and transient approaches, and the transient analysis proves to be crucial for understanding the squirrel cage IM's response to sudden changes and for validating its performance beyond steady-state operation.

The electromagnetic torque and currents at rated speed of the squirrel cage IM discussed in this paper shows close agreement between the steady-state predictions discussed in [Syed, Q.A.S., et. al. 2025]. The steady-state model for a slip of 0.032 predicted an electromagnetic torque of 24.13 N.m at 0 sec., whereas the transient model provides 26.2 N.m. Similarly, the current in the rotor bar at steady state model is 34.78 A, whereas transient model computes 34.77 A at 0 sec., and current in the stator winding at steady state model is 6.7 A, whereas transient model computes 6.13 A at 0 sec.

The squirrel cage IM is analyzed under the sequence of real-world events, including startup, loading, and fault conditions, offering critical insights into the IM's stability and response under varying operational demands. During the startup no load conditions, the squirrel cage IM's speed accelerates, and huge amount of the current is drawn, and electromagnetic torque produces with high fluctuations, however motor stabilizes, current drawn is heavily reduced, and speed and electromagnetic torque changes slightly.

When load is applied to the squirrel cage IM, the speed slightly reduces, and the current and electromagnetic torque rises and stabilizes to the new operating point. Under fault condition of a single-

phase short circuit with the neutral, the speed of the squirrel cage IM slightly increases with fluctuations, and peak values of the electromagnetic torque as well as current increases with unwanted oscillations.

Acknowledgement

Corresponding author acknowledges the support of Altair® for the 3D FEA license during the PhD research at the chair of Electrical Drives and Machines, FAU University of Erlangen-Nuremberg. The simulation and technical process is adopted from the Flux 2D solver manual.

References:

- [1] Syed, Q.A.S., Laghari, I.A., Ali, A., Samo, K.A., & Soomro, Z. (2025). Steady state electromagnetic analysis of the squirrel cage induction motor. *Spectrum of Engineering Sciences*. In parallel publication process.
- [2] El-Shahat, A., Ali, D., Thirugnanam, P., Tran, T., Brandštetter, P., Kuchař, M., Omar, F., Islam, A. S., Adib, A., Dhaouadi, R., Habibullah, T., Debanath, H., Sabbir, A. K. M., Belbali, S., Makhloufi, A., Kadri, L., Abdallah, Z., Seddik, Y., Zorgani, S., Hajji, Y., Koubâa, M., Boussak, S., Toumi, M., Benbouzid, M., Mimouni, S., Dabour, M., Hussien, A. M., Aboushady, M., Sen, K. K., Tran, T. C., Islam, A., Islam, A., Habibullah, M., Debanath, T., & Sabbir, M. S. H. (2023). *Induction motors - Recent advances, new perspectives and applications*. IntechOpen. <https://doi.org/10.5772/intechopen.104031>
- [3] Lipo, T.A. (2017). *Introduction to AC machine design*. Wiley. <https://doi.org/10.1002/9781119352181>
- [4] Boldea, I., & Nasar, S. A. (2010). *The induction machine handbook*. CRC Press, Taylor & Francis Group.
- [5] Kovács, K. (2022, September 5). Influence of the rotor slot numbers on the parasitic torques and the radial magnetic forces of the squirrel cage induction motor: An analytic approach. *International Conference on Electrical Machines*, Valencia, Spain. <https://doi.org/10.1109/ICEM51905.2022.9910>

- [6] Bleizgys, V., & Baskys, A. (2010). The influence of supply voltage amplitude variation law on AC induction motor efficiency in variable-speed drive. *Solid State Phenomena*, 164, 1-6. <https://doi.org/10.4028/www.scientific.net/SSP.164.1>
- [7] Azab, M. (2025). A review of recent trends in high-efficiency induction motor drives. *Vehicles*, 7(1), 15. <https://doi.org/10.3390/vehicles7010015>
- [8] Ahmed, S., Aarniovuori, L., Nerg, J., Barta, J., & Vitek, O. (2025). Emerging trends in high-speed induction machines and converter technologies for industrial applications. In *2025 IEEE International Electric Machines & Drives Conference (IEMDC)* (pp. 409-414). IEEE. <https://doi.org/10.1109/IEMDC60492.2025.11061054>
- [9] Balamurugan, S., Arumugam, R., Paramasivam, S., & Malaiappan, M. (2004, November). *Transient analysis of induction motor using finite element analysis*. Paper presented at the Conference of the Industrial Electronics Society, South Korea. <https://doi.org/10.1109/IECON.2004.1431805>
- [10] Zhang, D., Liu, T., He, C., & Wu, T. X. (2018). A New 2-D Multi-Slice Time-Stepping Finite Element Method and Its Application in Analyzing the Transient Characteristics of Induction Motors Under Symmetrical Sag Conditions. *IEEE Access*, 6, 51433-51443. <https://doi.org/10.1109/ACCESS.2018.2867277>
- [11] Altair Engineering, Inc. (2025). *Altair Flux 2D* [Finite element software for low-frequency electromagnetic and thermal simulations]. <https://altair.com/flux>
- [12] Di Nardo, M., Marfoli, A., Degano, M., Gerada, C., & Chen, W. (2020). Rotor design optimization of squirrel cage induction motor - part II: Results discussion. *IEEE*, 1-9. <https://doi.org/10.1109/TIE.2019.2922094>